



**HAL**  
open science

# Transferring bulk chemistry to interfacial synthesis of TFC-membranes to create chemically robust poly(epoxyether) films

Rhea Verbeke, Wouter Arts, Elke Dom, Marcel Dickmann, Werner Egger, Guy Koeckelberghs, Anthony Szymczyk, Ivo F. J. Vankelecom

## ► To cite this version:

Rhea Verbeke, Wouter Arts, Elke Dom, Marcel Dickmann, Werner Egger, et al.. Transferring bulk chemistry to interfacial synthesis of TFC-membranes to create chemically robust poly(epoxyether) films. *Journal of Membrane Science*, 2019, 582, pp.442-453. 10.1016/j.memsci.2019.02.016 . hal-02149781

**HAL Id: hal-02149781**

**<https://univ-rennes.hal.science/hal-02149781>**

Submitted on 8 Jul 2019

**HAL** is a multi-disciplinary open access archive for the deposit and dissemination of scientific research documents, whether they are published or not. The documents may come from teaching and research institutions in France or abroad, or from public or private research centers.

L'archive ouverte pluridisciplinaire **HAL**, est destinée au dépôt et à la diffusion de documents scientifiques de niveau recherche, publiés ou non, émanant des établissements d'enseignement et de recherche français ou étrangers, des laboratoires publics ou privés.

## Transferring bulk chemistry to interfacial synthesis of TFC-membranes to create chemically robust poly(epoxyether) films

*Rhea Verbeke,<sup>a</sup> Wouter Arts,<sup>a</sup> Elke Dom,<sup>a</sup> Marcel Dickmann,<sup>b</sup> Werner Egger,<sup>c</sup> Guy Koeckelberghs,<sup>d</sup> Anthony Szymczyk,<sup>e</sup> Ivo Vankelecom<sup>a,\*</sup>*

<sup>a</sup> Centre for Surface Chemistry and Catalysis, Faculty of Bioscience Engineering, KU Leuven, Celestijnenlaan 200F, PO Box 2461, 3001 Leuven, Belgium

<sup>b</sup> Heinz Maier-Leibnitz Zentrum (MLZ) and Physik Department E21, Technische Universität München, Lichtenbergstraße 1, 85748 Garching, Germany

<sup>c</sup> Institut für Angewandte Physik und Messtechnik, Universität der Bundeswehr München, 85577 Neubiberg, Germany

<sup>d</sup> Laboratory for Polymer Synthesis, Faculty of Chemistry, KU Leuven, Celestijnenlaan 200F, 3001 Leuven, Belgium

<sup>e</sup> Univ Rennes, CNRS, ISCR (Institut des Sciences Chimiques de Rennes) – UMR 6226, F-35000 Rennes, France

**Keywords:** nanofiltration; interfacial initiation of polymerization; poly(epoxyether); chlorine-resistance; extreme conditions; TFC-membranes

**Abstract:** Membrane technology is currently still excluded from separations in more aggressive feeds due to limited chemical robustness. To extent its applicability, a novel thin-film composite (TFC) membrane was synthesized via the homopolymerization of epoxide monomers, resulting in robust poly(epoxyether) top-layers with >90% rose bengal (MW = 1017 Da) and 70% methyl orange (MW = 327 Da) retention with reasonable water fluxes (>2 Lm<sup>-2</sup>h<sup>-1</sup>bar<sup>-1</sup>). The superior chemical stability of this novel nanofiltration membrane type was proven via treatments in pH 1 and 500 ppm NaOCl (pH 4) for, respectively, 48 h and 2.5 h, after which an unchanged or even improved membrane performance was observed. Additionally, the synthesis of the thin top-layer occurred via an interfacial initiation of the polymerization (IIP), rather than via state-of-the-art interfacial polymerization (IP). This IIP approach allowed to convert well-known monophasic bulk epoxide polymerization (commonly used in e.g. the automotive and coating industry), into the synthesis of thin, yet cross-linked top-layers.

## 1. Introduction

The popularity of membrane technology compared to traditional industrial separation techniques, such as distillation, adsorption and extraction, has strongly increased over the past decades, thanks to several environmental and economic benefits it has to offer. Thanks to so-called thin-film composite (TFC) membranes, consisting of an ultra-thin (<200 nm), yet dense selective layer on top of a porous support, water fluxes and high solute retentions are concurrently achieved [1–4]. The state-of-the-art synthesis technique for TFC-membrane is interfacial polymerization (IP), allowing the reaction between two monomers (often *m*-phenylene diamine (MPD) and trimesoyl chloride (TMC)) at the interface of two immiscible liquids [3,5].

TFC-membranes dominate the current nanofiltration (NF) and reverse osmosis (RO) market for (waste) water treatment and desalination. However, their applicability in more aggressive feeds, e.g. waste streams from chemical and pharmaceutical industries, acid leachates from the mining industry and chlorinated water streams from desalination, is limited due to their overall limited chemical robustness. Provided the enormous growth potential of membrane technology in these industries, there is an ongoing quest to obtain solvent-, pH- and chlorine-stable (TFC) membranes, which are additionally performing well in terms of retention and permeance [6].

In this work, the well-known epoxy resin bulk-chemistry, yet unexplored in membrane technology, is proposed to form new top-layers for TFC-membranes with enhanced stability, hence broader applicability. Epoxy resins are thermosetting and can be formed via different ways. When the epoxides react through a nucleophilic ring-opening polymerization (NROP) via a wide range of co-reactants, including amines, acids and acid anhydrides, an alkanolamine network is formed. Another possibility is to react through an anionic ring-opening polymerization (AROP), being actually a homopolymerisation. This reaction is initiated by, amongst others, tertiary amines [7] and results in a resin with polyether network chains [8]. Thanks to the inert ether bonds present in the latter [9], an exceptional stability towards bases, oxidizing and reducing agents, as well as stringent acidic conditions is in principle expected [10]. Additionally, the fact that ethers are often used as solvents for many organic reactions [9], makes these polyether networks interesting future candidates for Solvent-Resistant NF (SRNF) [11], Solvent-Tolerant NF (STNF) [12] or Organic Solvent Nanofiltration (OSN) [6] applications as well. However, these polymers are challenging to be applied as selective membrane layer, since their cross-linked forms, which are required with respect to membrane stability, cannot be dissolved anymore after synthesis. As a consequence, top-layer synthesis for TFC-membranes via dip- or spin-coating is impossible.

Herein, this issue was addressed by performing the AROP *in-situ* on a porous support by initiating the homopolymerisation of the epoxy monomer at the interface of two immiscible solvents. Similar to conventional IP, the epoxy monomer is dissolved in an apolar phase (toluene), while the initiator is dissolved in the aqueous phase within the support pores. When both phases are brought in contact, the reaction is believed to be initiated at the interface and to subsequently proceed in the organic phase. The initiator is thus not repeatedly incorporated

in the polymer network (as opposed to conventional MPD/TMC IP systems, where the monomers of both phases react with each other). This reaction, further denoted as ‘interfacial initiation of polymerization’ (IIP), yields selective poly(epoxyether) top-layers (**Figure 1**).

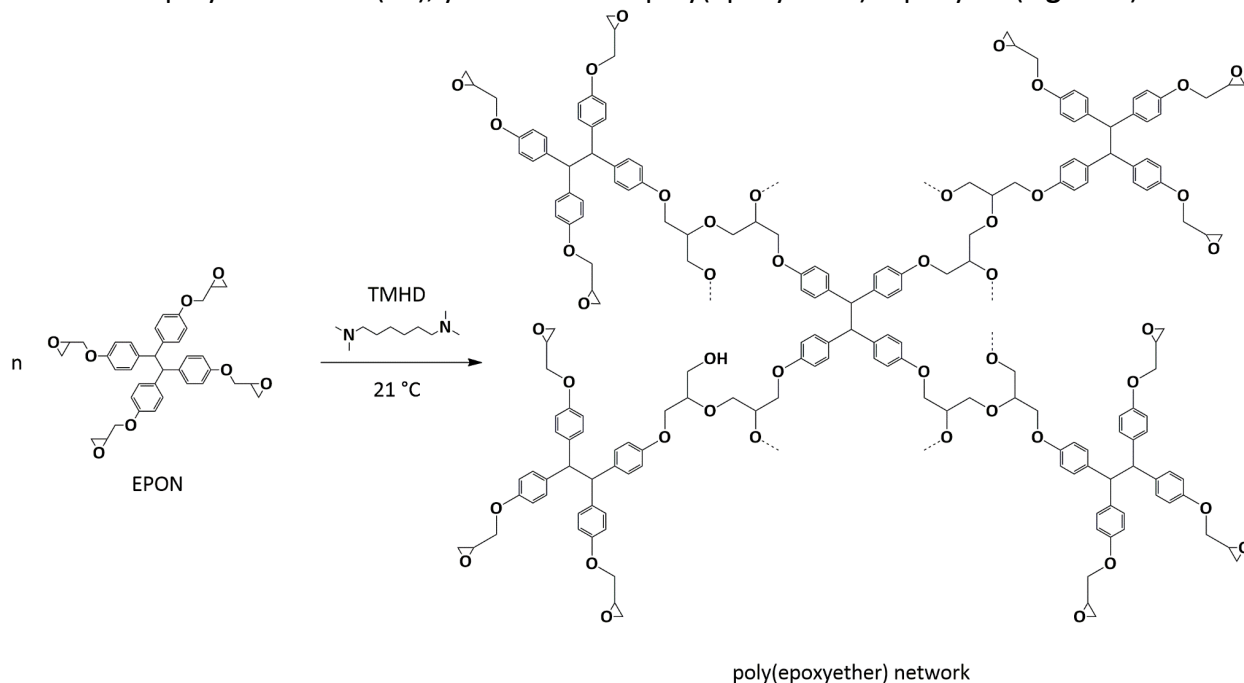


**Figure 1.** Hypothesized anionic ring-opening polymerization (AROP) of poly(epoxyether), starting from EPON (EPON™ Resin 1031, tetraphenoylethane tetraglycidylether) as epoxy monomer with TMHD (*N,N,N',N'*-Tetramethyl-1,6-hexanediamine) as initiator. The hydroxyl group in the network originates from the initiation step, believed to be produced via the acid-base reaction with the initiator.

Mechanisms for the AROP of epoxy monomers, initiated by tertiary amines, have been extensively discussed [13,14]. The assumed chain-growth polymerization comprises an initiation (1a and 1b), a propagation (2) and a termination step (3) (**Figure 2**). Two types of initiation steps are often hypothesized, wherein reaction 1a consists of the direct attack of the tertiary amine to the epoxy group, resulting in a zwitterion. Reaction 1b uses the presence of alcohols or other proton-donating (acids) compounds to obtain a highly reactive alkoxide ion. In this work, MQ-water, the solvent of the initiator, is believed to produce hydroxyl ions via the acid-base reaction with the initiator. Propagation will, by preference, be conducted through the nucleophilic attack of the alkoxide ions on the epoxy groups. Termination then occurs via reaction 3, wherein the solvent will again form alkoxides (or hydroxides in the case of water).

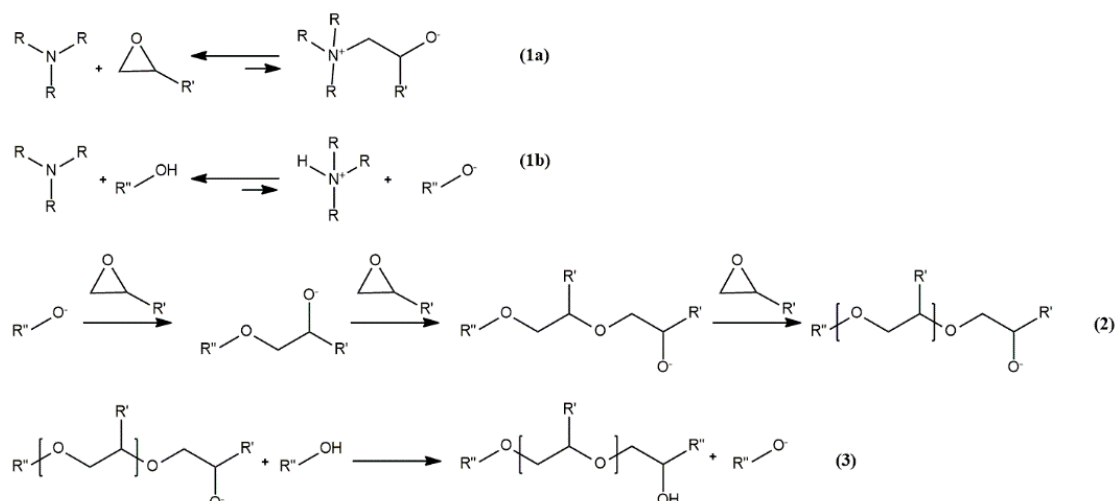


**Figure 2.** Epoxy homopolymerisation reaction mechanism initiated by a tertiary amine. Adapted from [13,14].

The main epoxy monomer used in this work is the tetra-functional, commercially available tetraphenolethane tetraglycidylether (EPON™ Resin 1031, further denoted as EPON). Its bulky structure with high epoxide equivalent weight (195 – 230 g/eq) [15] is believed to allow the formation of a relatively dense polymer network. BADGE (bisphenol A diglycidylether) is also used as bi-functional epoxy monomer to investigate its influence on the film-formation process. TMHD (*N,N,N',N'*-Tetramethyl-1,6-hexanediamine) is chosen as initiator of the homopolymerisation reaction due to its predicted high affinity for the organic phase thanks to the presence of six flexible methylene groups in its aliphatic chain, while still being soluble in water. The use of an amine with tertiary functionality is of high importance to avoid curing of the epoxy resin by the NROP, giving rise to the chemically less stable hydroxy-amine network. The proposed AROP reaction mechanism believed to occur in this work, which is thus initiated at the interface and subsequently proceeds in the organic phase, gives rise to the poly(epoxyether) top-layer (**Figure 1** and **Figure S1**).

To demonstrate the proof-of-concept of this new system, a parameter study was executed to obtain the optimum epoxy monomer concentration and reaction time. The synthesized membranes were characterized with ATR-FTIR, SEM, PALS, zeta potential and their performance was determined via filtration experiments. Secondly, to further shift the molecular weight cut-off (MWCO) curve to lower values, epoxy blends were explored. Further, the stability of the optimum membranes was assessed in extreme pH conditions (pH 1 and pH 13) and in an oxidizing environment (500 ppm NaOCl at pH 4).

## 2. Materials and Methods

### 2.1. Chemicals

The support layer was synthesized from polyimide (PI, P84©, Lenzing, Austria), non-woven polypropylene/polyethylene (PP/PE) fabric Novatexx 2471 (Freudenberg, Germany), tetrahydrofuran (THF, >99.9%, anhydrous and inhibitor-free, Sigma-Aldrich) and *N*-methyl-2 pyrrolidone (NMP, >99%, reagent grade, Honeywell) and 1,6-hexanediamine (HDA, 98%, Sigma Aldrich). The top-layer was synthesized from tetraphenolethane tetraglycidylether (EPON™

Resin 1031, Momentive, USA) and bisphenol-A-diglycidyl ether (BADGE, Sigma-Aldrich) as epoxy-resins, *N,N,N',N'*-Tetramethyl-1,6-hexanediamine (TMHD, 99%, Sigma-Aldrich) as initiator and toluene (99+%, extra pure, ACROS Organics) and Milli-Q (MQ) water (18.2 MΩ·cm at 25°C) as solvents. Rose Bengal (RB) sodium salt (1017 Da, Sigma Aldrich), methyl orange (MO, 327 Da, Fluka) and bromothymol blue sodium salt (BTB, 646 Da, Merck) were used as dyes for the filtration experiments. All chemicals were used as received.

## 2.2. Membrane synthesis

The cross-linked PI supports (XL-PI) were synthesized via immersion precipitation [16]. The polymer powder was dried overnight at 100°C before preparing a homogeneous solution of 14 wt% PI in NMP/THF 3:1. This solution was then cast on a PP/PE non-woven, which was impregnated with NMP, at constant speed (77 mm/s) using an automatic casting device (Braive Instruments, Belgium) at 250 μm wet thickness. 30 seconds after casting, the wet polymer film was immersed in distilled water at room temperature for 10 min. To synthesize a XL-PI, the support membrane was subsequently immersed for 1 h in a stirred aqueous amine solution of 1 wt% HDA to induce cross-linking [17]. The membrane was immersed in distilled water to allow diffusion of the unreacted HDA out of the support and subsequently stored in fresh distilled water until further use.

To synthesize the top-layer, interfacial initiation of polymerization was performed by immersing the porous cross-linked support in a 1 w/v% aqueous solution of TMHD for 1 h. Excess solvent was removed from the skin layer using a rubbery wiper. The membrane was horizontally fixed into a specially designed IIP set-up, after which a solution of an epoxy monomer (pure EPON, pure BADGE or a blend of both, with concentrations ranging from 0.1 to 3.5 w/v%) in toluene, was poured gently on the impregnated support, with the skin layer facing the epoxy solution. The set-up was then directly closed to avoid evaporation of toluene. After a specified reaction time, ranging from 30 to 240 min, the toluene solution was drained off, and the membrane was rinsed with toluene to remove unreacted epoxy monomers. The resulting poly(epoxyether) TFC-membrane was stored in distilled water until further use.

## 2.3. Membrane performance

The membrane performance was analyzed with a high-throughput filtration module which allows to run 16 simultaneous dead-end filtrations under exactly the same operating conditions [18]. The active area of each membrane coupon was  $1.77 \times 10^{-4} \text{ m}^2$ . To minimize concentration polarization, the feed was stirred at 350 rpm. Rose Bengal (RB, 35 μM), bromothymol blue sodium salt (BTB, 31 μM) or Methyl Orange (MO, 35 μM) in deionized water were used as feed solutions. The reported values (average and standard deviations) are based on at least 3 replicates (at least 3 coupons from at least one membrane sheet), unless stated otherwise. Furthermore, the optimal TFC membranes were filtrated with RB (35 μM) in deionized water during 70 h in order to assess their long term performance.

The permeance ( $\text{L m}^{-2} \text{h}^{-1} \text{bar}^{-1}$ ) was calculated using:

$$\text{Permeance} = \frac{V}{A \cdot t \cdot \Delta P}$$

with  $V$  (L) the permeate volume,  $A$  ( $m^2$ ) the membrane area,  $t$  (h) the filtration time and  $\Delta P$  (bar) the applied pressure. The retention (%) was calculated using:

$$\text{Retention} = \frac{C_f - C_p}{C_f}$$

with  $C_f$  and  $C_p$  the solute concentration in feed and permeate, respectively. The dye concentration was determined with UV-Vis absorption measurements (UV-1800, Shimadzu, UV Spectrophotometer) at 548 nm for RB, at 615 nm for BTB and at 457 nm for MO.

## 2.4. Physico-chemical membrane characterization

### 2.4.1. ATR-FTIR

The chemical composition of dried membrane surfaces was analyzed with attenuated total reflectance Fourier-transformed infrared spectroscopy (ATR-FTIR). A Bruker Alfa ATR-FTIR with a diamond crystal was used to collect 23 scans for each measurement at a resolution of  $3\text{ cm}^{-1}$ . Each membrane was measured at different positions to account for intra-sample variations.

### 2.4.2. SEM and TEM

The morphologies of the top-layers were analyzed by scanning electron microscopy (SEM) using a Philips XL30 FEG instrument. The samples were sputter coated with 5 nm of Pt before the analysis. Several images at different magnifications were taken of each sample to account for intra-sample variations.

Membrane samples for analysis with transmission electron microscopy (TEM) were first embedded in an Araldite® resin (Polyscience) and subsequently cut into very thin cross-section slices (70 nm) with a Leica EM UC6 microtome. Images were taken with a Zeiss EM900 microscope.

### 2.4.3. Zeta potential

Tangential streaming current measurements were carried out with an electrokinetic analyzer (Surpass 3, Anton Paar GmbH, Austria). Two identical rectangular membrane samples (2 cm x 1 cm) were fixed on sample holders using double-sided adhesive tape and the distance between the samples was set to  $100 \pm 5\ \mu\text{m}$  for all measurements. The streaming current generated along the membrane surfaces was measured with Ag/AgCl electrodes for pressure ramps of 400 mbar. Membrane samples were soaked overnight into the measuring solution (0.001 M KCl) prior to measurements (performed at room temperature, i.e.  $19 \pm 1\ ^\circ\text{C}$ ). The zeta potential was inferred from the standard Smoluchowski equation.

### 2.4.4. PALS

Positron annihilation lifetime spectroscopy (PALS) is able to measure free volume in polymer membranes and was applied in this work under the same conditions as previously reported by our group [19]. In brief, the ortho-positronium (o-Ps) can get trapped inside the free-volume elements of the polymer, until it annihilates with the surroundings. The so-called pick-off lifetime can be correlated to the size of the free-volume elements by the Tao-Eldrup model [20,21]. Additionally, the intensity of the o-Ps lifetime component can be used, in some cases, to estimate relative changes in free volume abundance. The lifetime spectra were measured

with the Pulsed Low Energy Positron Beam System (PLEPS), operated at the neutron induced positron source Munich (NEPOMUC) [22–25].

Implantation energies of 1 keV were used, corresponding to median implantation depths of ca. 30 nm, assuming a polymer density of 1 g/cm<sup>3</sup> [26]. For these spectra, 4 million counts were collected with a counting rate of about 10 000 cts/s and the time resolution was ca. 250 ps. The resolution function was determined by measuring p-doped SiC. The spectra were deconvoluted into four lifetime components (p-Ps, free e<sup>+</sup> and two o-Ps) with PALSfit3 [27], leading to overall fit variances below 1.2.

### 3. Results and Discussion

#### 3.1. EPON-based TFC-membranes

##### 3.1.1. EPON-concentration optimization

##### 3.1.1.1. Filtration results

An optimization of the EPON-concentration was performed to assess the minimum concentration needed to achieve a RB retention of at least 90% in water for a reaction time of 1 h. The XL-PI support had a permeance of 111.2 ( $\pm 16.4$ ) Lm<sup>-2</sup>h<sup>-1</sup>bar<sup>-1</sup>, with a RB retention of only 51.0 ( $\pm 9.8$ )%. After performing IIP during 1h with various concentrations of EPON, all resulting TFC-membranes achieved higher RB retentions and were less permeable than the XL-PI support (**Figure 3**). A maximum RB retention of 89.5 ( $\pm 3.4$ )% was attained at an EPON-concentration of 1.5 w/v%, together with a reasonable water permeance of 2.1 ( $\pm 1.5$ ) Lm<sup>-2</sup>h<sup>-1</sup>bar<sup>-1</sup>. The RB retention did not increase further with increasing EPON-concentration, even though the water permeance did drop significantly. This suggests that a thicker, though not denser selective layer was formed. The optimum EPON-concentration for a 1 h reaction time was hence found to be 1.5 w/v%.

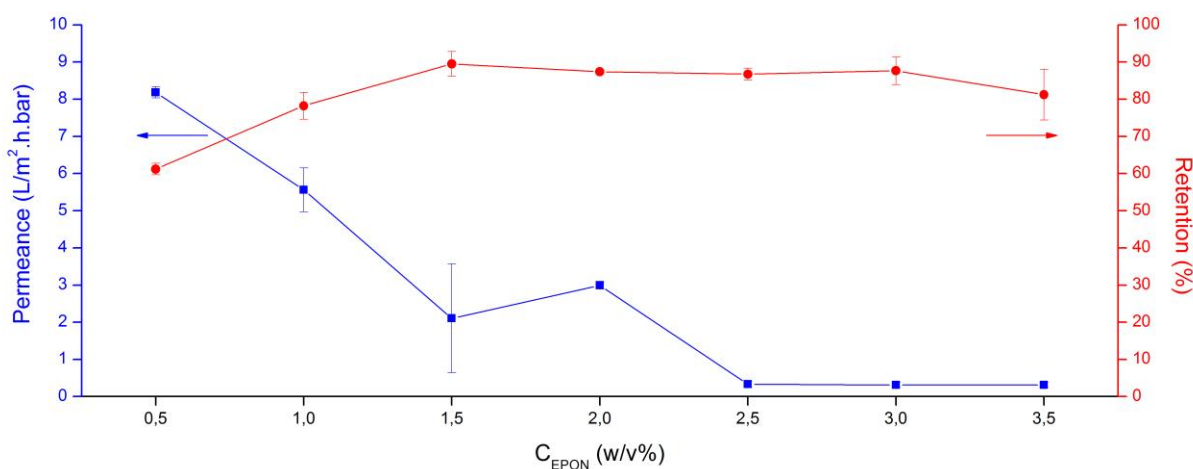


**Figure 3.** Water permeance and RB retention as a function of EPON-concentration in the organic phase. TMHD concentration was kept constant at 1 w/v% and reaction time set at 1 h.

Filtration conditions: 25°C, 10 bar, 35  $\mu\text{M}$  RB in deionized water. Averages based on at least 3 replicates.

### 3.1.1.2. ATR-FTIR

ATR-FTIR was used to characterize the chemical bonds in both the pristine support membrane and the TFC-membranes synthesized with different EPON-concentrations. Additionally, a free-standing poly(epoxyether) film (*i.e.* synthesized in biphasic bulk system without support) was used as reference to localize the typical bonds associated with the top-layer. Regarding the XL-PI support, all characteristic absorption peaks are present (**Figure 4**), in agreement with [17]. The amide peaks, present at  $1640\text{ cm}^{-1}$  (C=O stretch of secondary amide) and  $1525\text{ cm}^{-1}$  (N-H bending of secondary amide) [28] indicate cross-linking. However, also primary amine bends ( $1600\text{ cm}^{-1}$ ), C=O imide stretches ( $1780$  and  $1711\text{ cm}^{-1}$ ) and C-N imide stretches ( $1364\text{ cm}^{-1}$ ) are present [29], indicating that cross-linking was not complete, though sufficient to ensure stability of the cross-linked support in toluene (*i.e.* the organic solvent used during IIP). The gradual decline of these support-related peaks with increasing EPON-concentration suggests that, just like the filtration results, a thicker top-layer is formed at higher EPON-concentrations. Additionally, the emerging peaks in the spectra of the TFC-membranes around  $1500\text{ cm}^{-1}$  and between  $1200$  to  $700\text{ cm}^{-1}$  further grow in intensity at higher concentrations and are believed to originate from the top-layer, as they overlap with the free-standing poly(epoxyether) film (**Figure S2**). The latter is characterized by peaks corresponding to the asymmetric C-O-C stretch of aliphatic ethers ( $1150 - 1080\text{ cm}^{-1}$ ), as well as to the asymmetric and symmetric C-O-C stretch of aryl alkyl ethers ( $1275 - 1200\text{ cm}^{-1}$  and  $1075 - 1020\text{ cm}^{-1}$ ) [28]. The strong peak around  $1520\text{ cm}^{-1}$  most probably originates from the benzene moieties in EPON [30]. ATR-FTIR thus also qualitatively demonstrates the successful formation of a poly(epoxyether) top-layer via IIP on a XL-PI support.

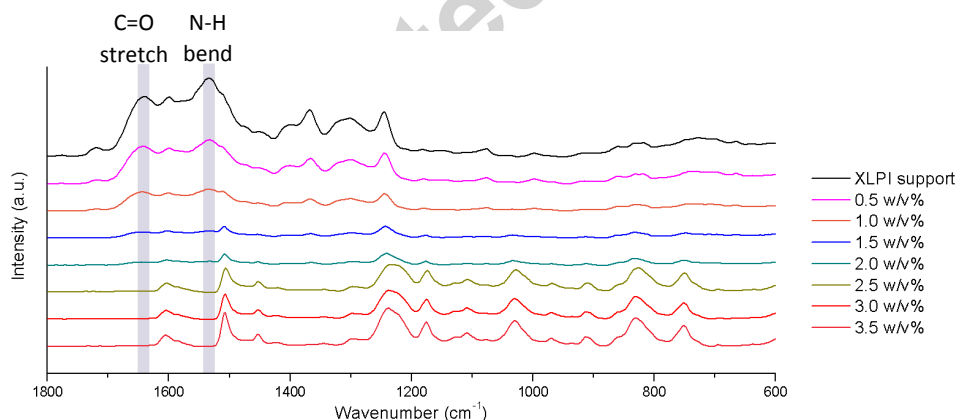


**Figure 4.** Representative ATR-FTIR spectra of the XL-PI support and the TFC-membranes, synthesized with different EPON-concentrations in toluene (1 h reaction time, 1 w/v% TMHD). The C=O stretch and N-H bend of secondary amides, originating from the partially XL-PI support, are indicated.

### 3.1.1.3. SEM and TEM

When comparing top-view SEM images from the uncoated support with those from the IIP-synthesized TFC-membranes, a completely different morphology is observed (**Figure 5**). The relatively smooth XL-PI support gets covered with sphere-like structures after IIP has occurred. At 0.5 w/v% EPON, these structures are less pronounced, however, with increasing EPON-concentration, the spheres grow in size, ranging from roughly 0.9  $\mu\text{m}$  at 1 w/v% to 2.5  $\mu\text{m}$  at 2 w/v%, based on SEM-images (**Figure 6**). At even higher EPON-concentrations, a more net-like structure emerges, supposed to originate from spheres which have grown towards each other in the plane of the membrane (*i.e.* in the x- and y-direction), until the surface completely flattens out again. The lower permeabilities and lower intensities of the support-related ATR-FTIR peaks at higher EPON-concentrations are thus believed to originate from a top-layer which is thicker (perpendicular to the membrane, *i.e.* z-direction) and/or from a top-layer which covers the support layer in a more homogeneous way (x- and y-direction).

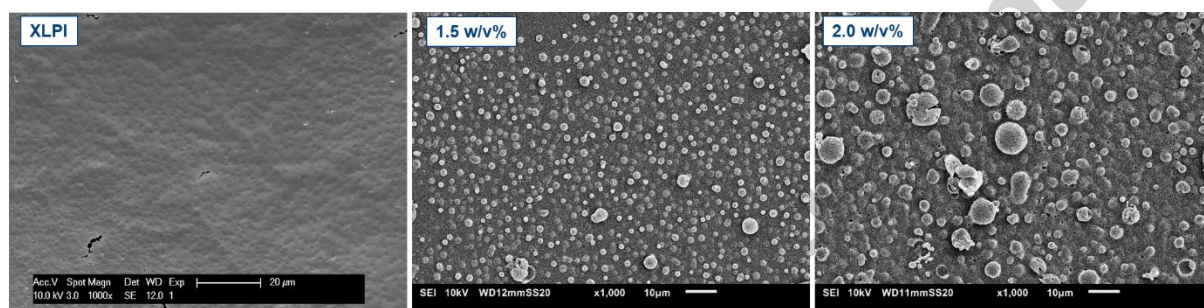


**Figure 5.** SEM top-view images of the XL-PI support and from IIP-synthesized TFC-membranes with 1.5 and 2 w/v% EPON in toluene (1 h reaction time, 1 w/v% TMHD).

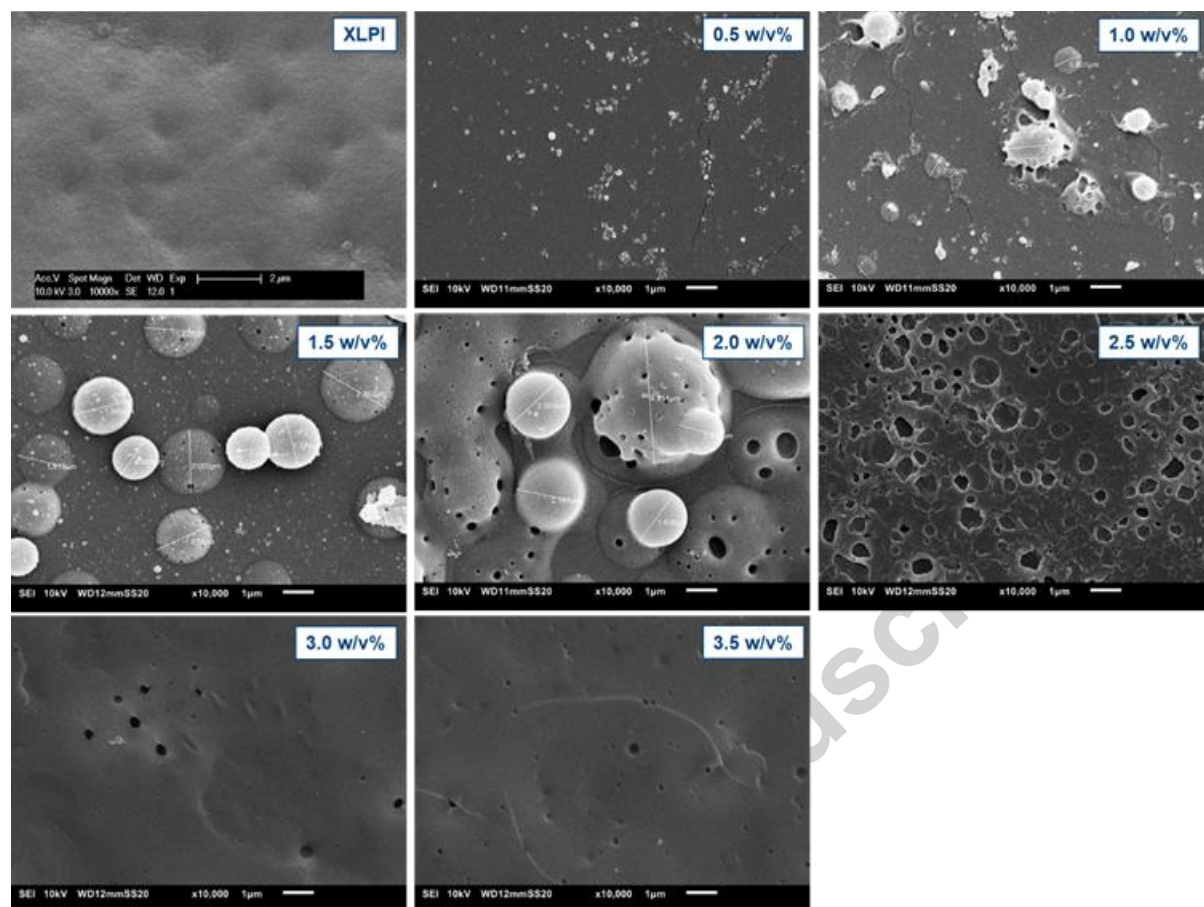


**Figure 6.** Top-view SEM images of the XL-PI support and of IIP-synthesized TFC membranes with varying concentration of EPON in toluene (1 h reaction time, 1 w/v% TMHD).

Cross-section TEM images were taken to quantitatively determine the top-layer thickness. However, no top-layer was visible on any of the IIP-synthesized TFC-membranes (**Figure S3**). This is believed to be due to the low contrast between the Araldite<sup>®</sup> resin, in which the samples are embedded during sample preparation, and the poly(epoxyether) top-layer, as their chemical compositions are very similar.

### 3.1.2. Reaction time optimization

From the above experiments, the optimum EPON-concentration in toluene to synthesize poly(epoxyether) TFC-membranes lies at 1.5 w/v% for 1 h reaction time. The next aim was to investigate whether the reaction time could be decreased at this optimum EPON-concentration, while still maintaining a selective membrane for RB. Longer reaction times were additionally tested in order to get a better understanding of the film-formation process.

#### 3.1.2.1. Filtration results

An IIP reaction time ranging from 5 to 30 min is insufficient to obtain a selective NF membrane (**Figure 7**). However, the results do suggest that a reaction occurred, as the water permeances are significantly lower compared to the uncoated XL-PI support ( $111.2 (\pm 16.4) \text{ Lm}^{-2}\text{h}^{-1}\text{bar}^{-1}$ ). When increasing the reaction time from 30 to 60 min, the RB retention strongly

increases and the water permeance drops. When further increasing the reaction time to 240 min, a slightly higher RB retention is achieved (91.1 ( $\pm 1.5$ )%), while the permeance does not drop significantly. The optimal reaction time is thus 1h. The retention of the optimal membrane for smaller dyes than RB, namely BTB and MO, was also measured (**Table 1**). A gradual, but small, decrease in retention with decreasing solute size was observed. However, a retention of 70 % for MO, a dye of only 327 g/mol, was still achieved.

**Table 1.** Retention of the optimal EPON-based membrane (1.5 w/v% EPON, 1 w/v% TMHD, 1 h reaction time) for 3 different dyes (RB, BTB and MO).

Dye	MW (g/mol)	Retention (%)	
		EPON-based	EPON/BADGE-based
RB	1017.64	89.50 $\pm$ 3.40	95.20 $\pm$ 0.50
BTB	646.36	84.46 $\pm$ 3.19	73.25 $\pm$ 14.29 *
MO	327.33	70.26 $\pm$ 5.19	70.30 $\pm$ 1.50

\* Based on 2 coupons

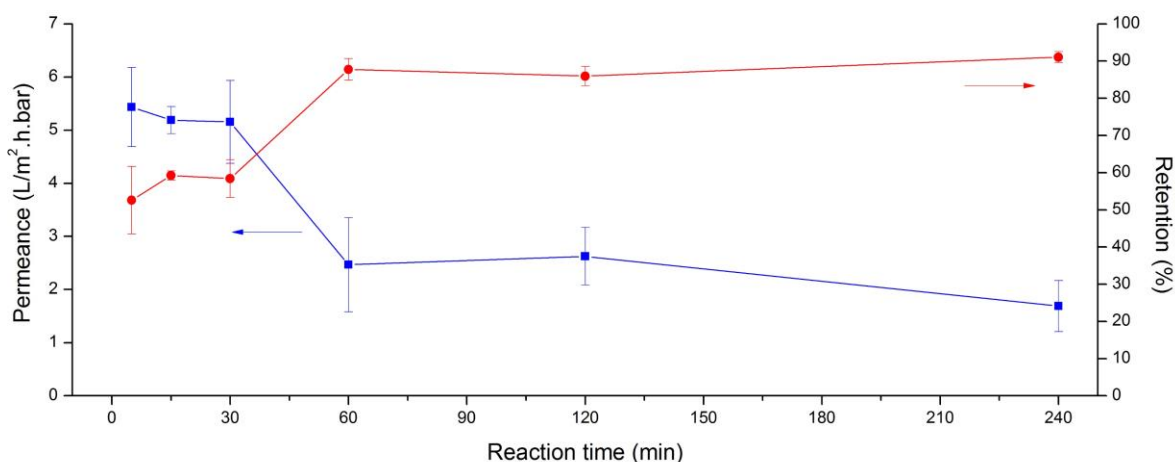


**Figure 7.** Water permeance and RB retention as a function of reaction time for a constant EPON in toluene concentration (1.5 w/v%) and a 1 w/v% TMHD concentration. Filtration conditions: 25°C, 10 bar, 35  $\mu$ M RB in deionized water. Averages based on at least 3 replicates.

Worth noting is the high reproducibility of the IIP-reaction at the optimum synthesis conditions. Separate batches of the 1.5 w/v% membrane, originating from both optimization studies, resulted in average RB retentions of 89.5 ( $\pm 3.4$ )% and 87.7 ( $\pm 2.9$ )% and average water permeances of 2.1 ( $\pm 1.5$ ) and 2.5 ( $\pm 0.9$ )  $\text{Lm}^{-2}\text{h}^{-1}\text{bar}^{-1}$ . The average RB retention of both batches (*i.e.* based on a total of at least 6 coupons from at least 2 membrane sheets) is hence 88.5 ( $\pm 3.0$ )%, with a water permeance of 2.3 ( $\pm 1.1$ )  $\text{Lm}^{-2}\text{h}^{-1}\text{bar}^{-1}$ . Besides their high reproducibility, the long term performance of these TFC membranes is also worth mentioning as their retention remained constant and their permeance did not significantly decrease during 70 h of filtration with RB in water (**Figure S4**). As a consequence, retention solely based on adsorption of RB on the membrane can be excluded. This observation is also substantiated by the gradual increase in RB concentration in the retentate (**Figure S5**).

As opposed to conventional IP, the IIP reaction is not self-quenching. Therefore, the reaction can theoretically continue until depletion of the epoxy monomer in the organic phase, provided that the active center of reaction is not inactivated (e.g. protonation of alkoxide). It was therefore expected that, with increasing reaction time, thicker top-layers are formed, resulting in lower permeances. As this is not the case, a thorough analysis via SEM imaging was executed to check whether different morphologies at higher concentrations are present.

### 3.1.2.2. SEM

Similar spherical structures as in **Figure 5**, which seem to grow in size with increasing reaction time, are again observed on the top-view SEM images of the TFC-membranes (**Figure 8**). At higher reaction times, the spheres appear more pronounced but are, remarkably, also more hollow. This is opposed to thin PA films, in which the hollow voids are either completely encapsulated by polymer strands or interconnected to the back surface (*i.e.* support side), but not to the feed side [31]. This observation can possibly explain why the permeance did not further decrease with increasing reaction time. Also, the size of the spherical structures present in the poly(epoxyether) film lies in the  $\mu\text{m}$ -range, while the protrusions present in the PA ridge-and-valley structure are a few nanometers big [31]. These differences again indicate the contrasting chemistry and reaction system of this work compared to conventional MPD/TMC-based IP.

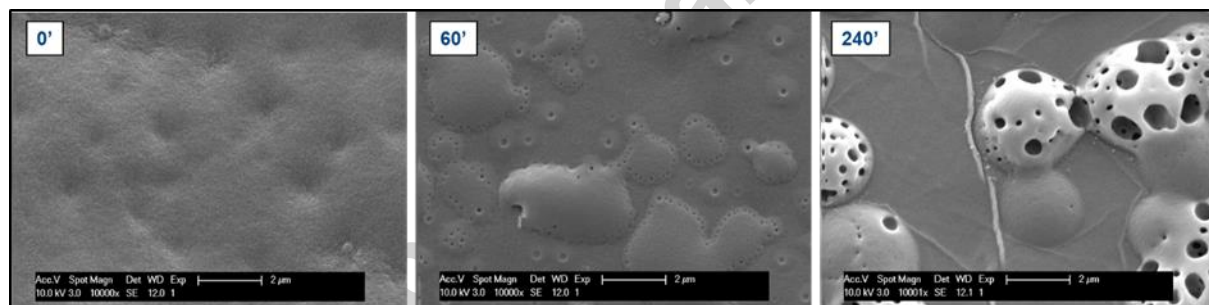


**Figure 8.** SEM top-view images of the XL-PI support (0') and from IIP-synthesized TFC-membranes with 1.5 w/v% EPON in toluene during 60 and 240 min reaction time (1 w/v% TMHD).

Cross-section SEM-images also reveal the presence of similar sphere-like structures at the surface of the poly(epoxyether) top-layer (**Figure 9**), which coincide in size with those of the top-view images. The top-layer thickness can also be roughly estimated from these images, even though care should be taken because of interference from the skin-layer of the support. Thicknesses around 200 nm are observed, depending on whether the extrusions are taken into account. An overall slightly thicker top-layer for the longest reaction time (roughly 260 nm), compared to a reaction time of 60 min (roughly 220 nm) (**Figure 9**) can tentatively be observed. This could also be deduced from the decreasing intensities of the chemical bonds related to the support-layer on the IR spectra (**Figure S6**). Therefore, as the permeance did not drop significantly with increasing reaction time, it is believed that mainly the hollow morphology of

the spheres can be accounted for this absent relationship between top-layer thickness and permeance.

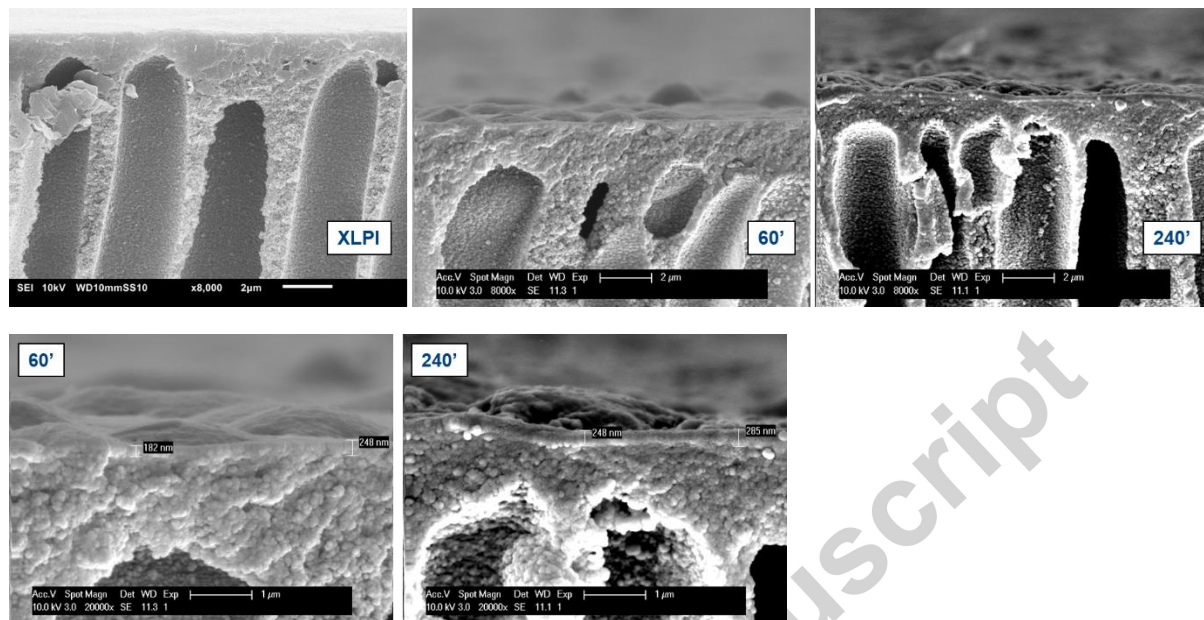


**Figure 9.** SEM cross-section images of the XL-PI support and IIP-synthesized TFC-membranes with 1.5 w/v% EPON in toluene during 60 and 240 min reaction time (1 w/v% TMHD). The estimated thickness of the top-layer of the 60' and 240' TFC membranes is shown on the images.

### 3.1.2.3. Zeta potential

The surface charge of the optimal EPON-based membrane was analyzed via zeta potential measurements. Surprisingly, the TFC membrane with poly(epoxyether) top-layer has a significant negative charge at pH values between 5 and 8 (**Figure 10**). The hypothesized chemical structure of the top-layer (**Figure 1**) would however not result in such a zeta potential curve, as the functional groups able to provide charge are terminal OH-groups, which are not deprotonated in this pH-range. Qualitatively similar results with respect to negative electrokinetic charge density for other polymers bearing no ionizable groups have been reported [32] and are expected to originate from specific adsorption of hydroxide ions from the feed on the membrane surface [33]. Additionally, there are no big changes in the zeta potential curves of the bare XL-PI support and the TFC membrane. It is therefore hypothesized that a substantial part of the streaming current flows through the porous, thick and charged XL-PI support of the TFC membrane. As a consequence, the obtained signal of the TFC membrane is thus also strongly influenced by its support and can therefore not solely be related to the surface charge of the poly(epoxyether) top-layer.

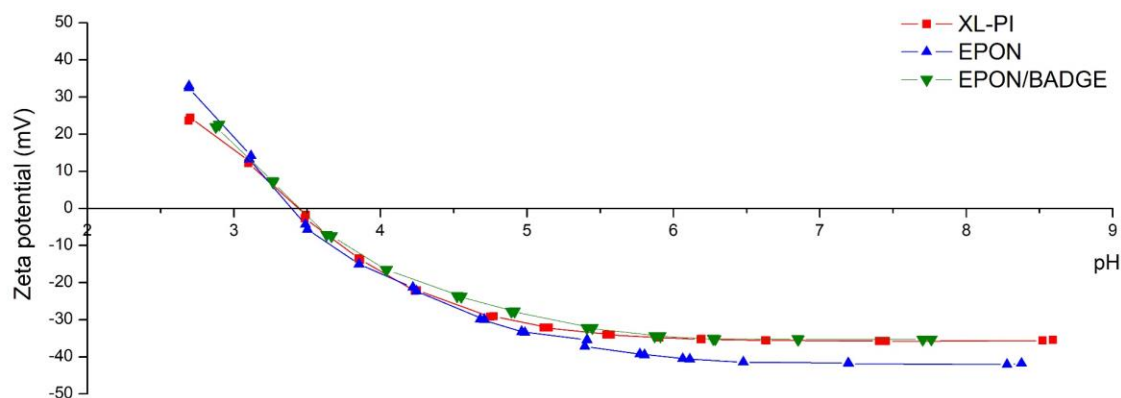


**Figure 10.** Zeta potential of the bare XL-PI support, the optimal EPON-based membrane (1.5 w/v% EPON, 1 w/v% TMHD, 1 h reaction time) and the optimal EPON/BADGE-based membrane (0.75/0.75 EPON/BADGE w/v%, 1 w/v% TMHD, 2 h reaction time).

### 3.2. EPON-BADGE-based TFC-membranes

The best performing membrane resulting from the optimization studies (*i.e.* 1.5 w/v% EPON, 1 h reaction time) achieved a RB retention of 88.5 ( $\pm$  3)% and is thus not capable of fully rejecting a dye of 1017 Da. It is expected that this is caused by the too large size of the free-volume elements present in the network due to the homopolymerisation of the bulky EPON monomer. Therefore, in order to decrease the MWCO, IIP was conducted by (partially) replacing EPON by the smaller BADGE monomer (**Figure 11**). BADGE is namely expected to create smaller free-volume elements and possibly also fill up the larger free-volume elements created through EPON polymerisation. First, the optimum ratio EPON/BADGE was investigated, followed by assessing the optimal reaction time.

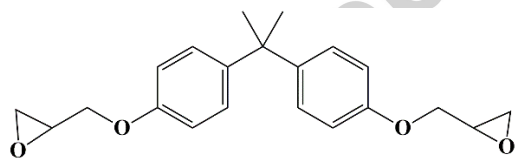


**Figure 11.** Chemical structure of bisphenol A diglycidylether (BADGE).

#### 3.2.1. Filtration results

The EPON/BADGE ratio was varied, while keeping the total amount of epoxy monomer constant at the optimized 1.5 w/v% to ensure that the number of functional epoxy groups and total epoxy mass remains constant. When replacing 50% of EPON by BADGE (*i.e.* using 0.75/0.75 EPON/BADGE w/v%) in the monomer solution, the permeance and RB retention of the epoxy-blended TFC-membranes remains similar to the optimal 1.5 w/v% pure EPON membrane (**Figure 12**). When further increasing the BADGE concentration in the monomer solution, the permeance and retention proportionally increase and decrease, respectively. These results indicate that BADGE is indeed incorporated in the top-layer, which results in

either a looser top-layer or in an incomplete coverage of the top-layer on the support layer during the unoptimized 1 h reaction time. All epoxy-blended top-layers nevertheless outperform the XL-PI support, opening enormous possibilities in tuning membrane performance by simply replacing or varying the epoxy monomer in the organic solution.

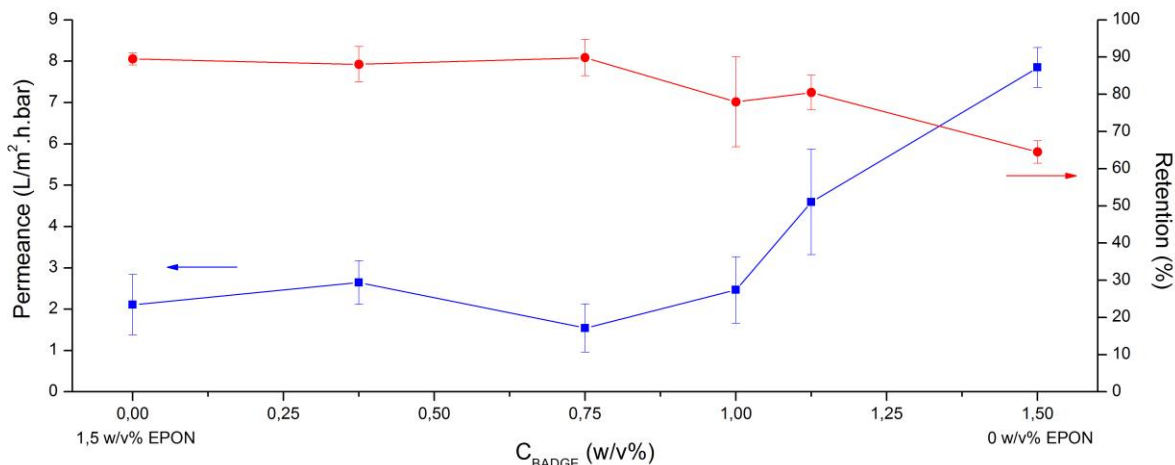


**Figure 12.** Water permeance and RB retention as a function of BADGE concentration. The total amount of epoxy monomers was kept constant at 1.5 w/v%, so that 0 w/v% BADGE corresponds to 1.5 w/v% EPON, and vice versa (1 h reaction time, 1 w/v% TMHD). Filtration conditions: 25°C, 10 bar, 35  $\mu\text{M}$  RB in deionized water. Averages based on at least 3 replicates.

When prolonging the reaction time for the optimized 0.75/0.75 EPON/BADGE w/v% membrane to 120 min, the RB retention reaches a maximum value of 95.2 ( $\pm 0.5$ )%, though at the expense of water permeance ( $0.6 (\pm 0.3) \text{ Lm}^{-2}\text{h}^{-1}\text{bar}^{-1}$ ) (**Figure 13**). Further increasing the reaction time does not result in an increase in membrane performance. The longer reaction time needed compared to the pure EPON-system is believed to be caused by the two times lower functionality of BADGE. The average RB retention of the 120 min (95.2 ( $\pm 0.5$ )%) EPON/BADGE-membranes is also slightly superior to that of the optimal EPON-based membrane (88.5 ( $\pm 3$ )%), most probably thanks to the beneficial combination of prolonged reaction time and possible insertion of BADGE in the epoxyether network during 2 h of reaction. On the other hand, the retention for MO and BTB of this membrane is similar to the optimal EPON-based membrane (**Table 1**), suggesting that the formed EPON/BADGE network is not dense enough to better reject smaller dyes than the pure EPON-based network. Additionally, the long term performance of the optimal EPON/BADGE-based membranes (0.75/0.75 EPON/BADGE w/v%, 1 w/v% TMHD, 2 h reaction time) remained constant during 70 h of filtration, in a similar manner as the pure EPON-based membranes (**Figure S7**).

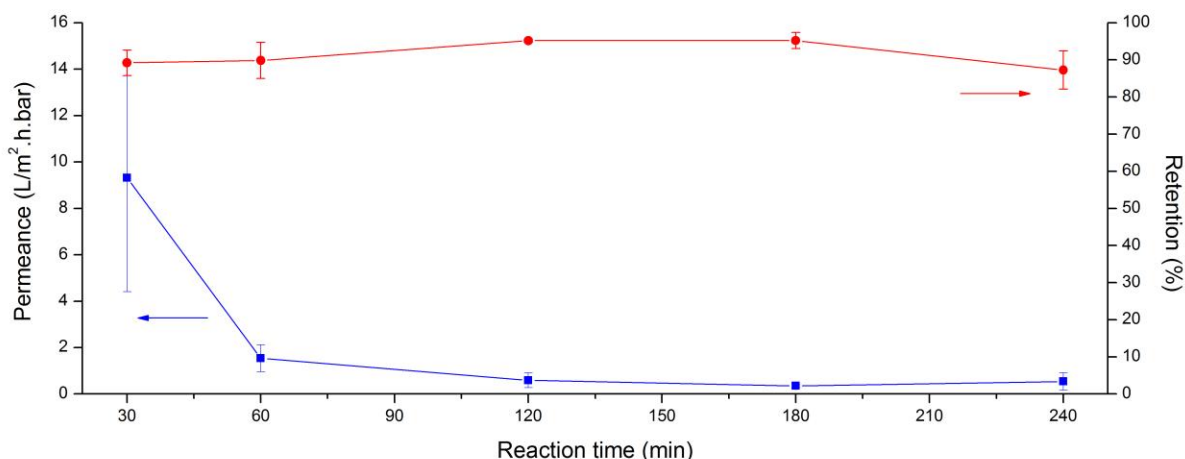


**Figure 13.** Water permeance and RB retention as a function of reaction time for a 0.75/0.75 EPON/BADGE w/v% in toluene solution (1 w/v% TMHD). Filtration conditions: 25°C, 10 bar, 35  $\mu$ m in deionized water. Averages based on at least 3 replicates.

### 3.2.2. ATR-FTIR

No change in ATR-FTIR spectra is observed between the pure EPON (0% BADGE) and the 25 or 50% EPON (**Figure 14**) for 1 h reaction time, in agreement with their similar filtration performance. However, with increasing BADGE concentration in toluene, the support-related peaks become more visible, suggesting that the top-layer is either less thick, less dense or that it does not fully cover the support. SEM and PALS are employed to substantiate these hypotheses. For the membranes synthesized with equal EPON and BADGE concentration (0.75/0.75 EPON/BADGE w/v%) and varying reaction times, the ATR-FTIR spectra also accord well with the filtration results (**Figure S8**). The support related bands decrease with increasing reaction time and vanish for the membrane obtaining the highest RB retention, while the characteristic top-layer peaks increase in intensity. Only for the membrane synthesized during 240 min, the support related peaks remain clearly present, assumed to result from a less homogenous top-layer, as also indicated by the slightly lower RB retention with higher standard deviations.

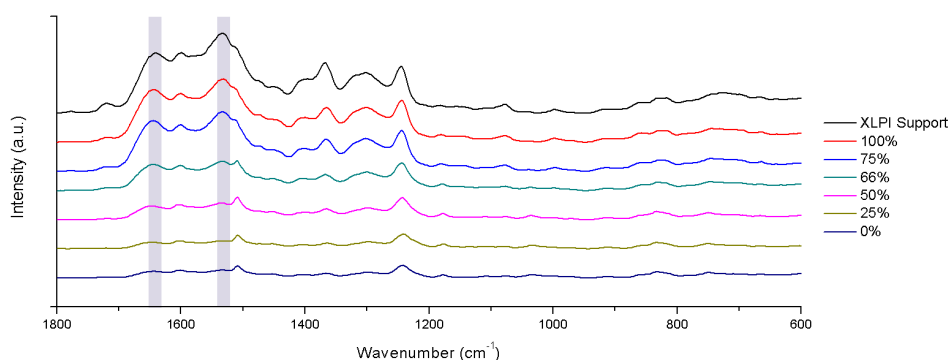


**Figure 14.** Representative ATR-FTIR spectra of the XL-PI support and the TFC-membranes, synthesized with varying EPON/BADGE ratios (1 h reaction time, 1 w/v% TMHD). The percentages shown indicate the BADGE% in a 1.5 w/v% epoxy solution (e.g. 50% indicates 0.75 w/v% BADGE with 0.75 w/v% EPON). The C=O stretch and N-H bend of secondary amides, originating from the partially XL-PI support, are indicated.

### 3.2.3. SEM

Top-view SEM images again show the emergence of spheres on the top-layer for the membranes synthesized with high EPON-concentrations. However, with increasing BADGE concentration in the organic solution, the number and size of these features decreases and their shape changes (**Figure 15**), suggesting that a different morphological network originates when the amount of bi-functional BADGE exceeds the tetra-functional EPON. For the pure BADGE membrane, the surface becomes almost flat, indicating that the sphere-like structures are a result from the EPON monomer in the synthesis of poly(epoxyether) top-layers. Higher magnification SEM images also do not reveal any holes or defects in the spheres of the BADGE-containing membranes (**Figure S9**), as some EPON-based membranes do. PALS was used to investigate whether, at molecular scale, the introduction of BADGE in the polymer network indeed resulted in the filling of the free-volume elements, which were generated by the bulky EPON building block.

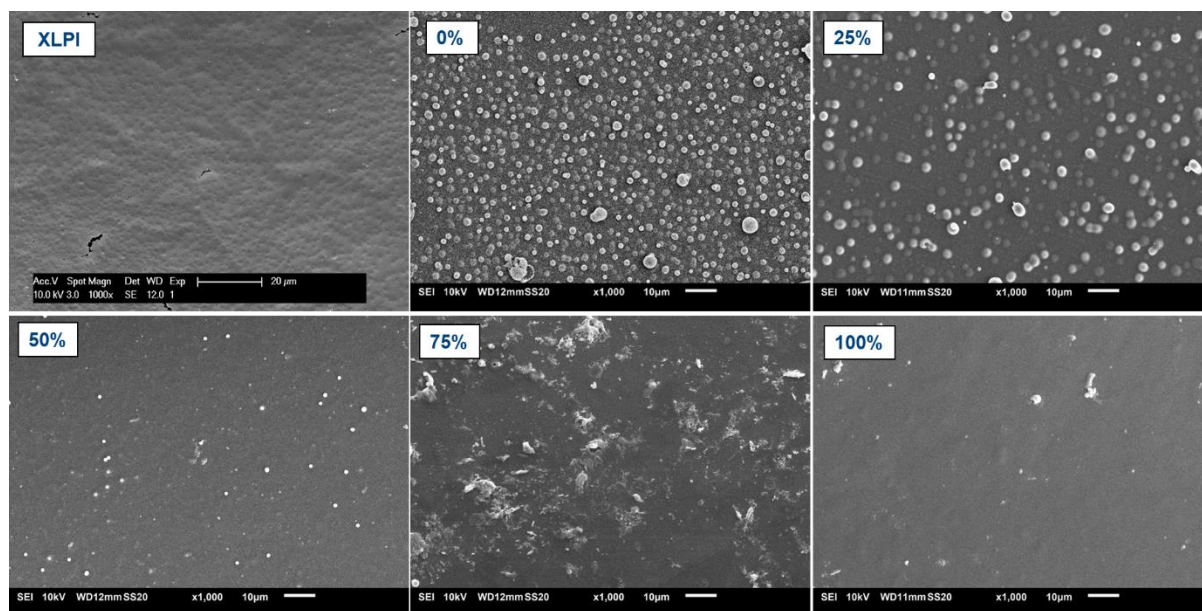


**Figure 15.** SEM top-view images of the XL-PI support and the TFC-membranes, synthesized with varying EPON/BADGE ratios (1 h reaction time, 1 w/v% TMHD). The percentages shown indicate the BADGE% in a 1.5 w/v% epoxy solution (e.g. 50% indicates 0.75 w/v% BADGE with 0.75 w/v%).

The (cross-section) SEM images from the reaction time optimization study of the 0.75/0.75 EPON/BADGE w/v% membranes again reveal spherical structures, which seem to flatten out at longer reaction times, to eventually merge after 180 min of IIP (**Figure 16** and **Figure S10**). The increased RB retention and decreased support-related IR-peaks hence nicely correlate with this change in morphology.

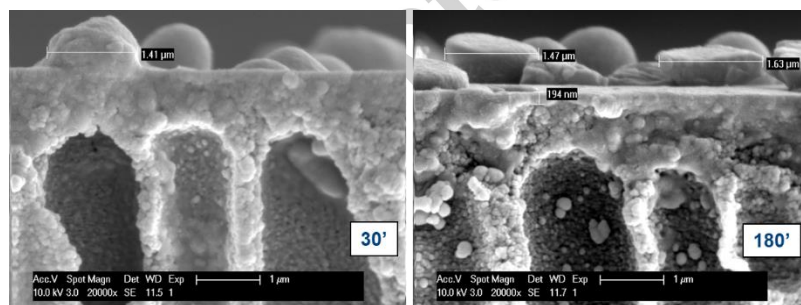


**Figure 16.** Cross-section SEM images of the XL-PI support and the TFC membranes, synthesized from a 0.75/0.75 w/v% EPON/BADGE in toluene solution (1 w/v% TMHD).

#### 3.2.4. Zeta potential

As for the pure EPON-based membrane, the zeta potential curve of the optimal EPON/BADGE-based membrane is nearly identical to that of the XL-PI support (**Figure 10**). As explained above, the substantial amount of streaming current originating from the support layer is believed to strongly influence the zeta potential curve of the TFC membrane, hence not allowing to differentiate between bare support and support coated with poly(epoxyether) top-layer.

Specific adsorption of hydroxyl ions from the aqueous feed might also be responsible for the similar zeta potential curves [33].

### 3.2.5. PALS

PALS was used to investigate whether the introduction of BADGE in the top-layer indeed resulted in differences in free-volume. According to the data fitting procedure, two different o-Ps components were observed in all spectra. In the following, these components will be labelled as the “short” and the “long” o-Ps lifetime component.

The “short” lifetimes of these samples are converted into free-volume hole radii via the Tao-Eldrup model [20,21]. The short o-Ps component follows a clear trend for the epoxy-blending series: a proportional increase in free-volume element radius with increasing BADGE concentration is observed (**Figure 17**). This trend clearly correlates with the filtration results (**Figure 12**): a lower retention and higher permeance correspond to bigger free-volume elements. The obtained results evidence that the size of free-volume element is indeed an important parameter with respect to transport through the top-layer, as expected from its presence in the diffusion coefficient in the solution-diffusion model [34]. It can thus be concluded that top-layers made with the tetra-functional EPON have significantly smaller free-volume elements in their top-layer (average size of 0.51 nm), compared to pure BADGE-based membranes (average size of 0.58 nm). PALS could thus quantitatively reject the hypothesis that BADGE fills up the free-volume present in the EPON-based network when the IIP lasts for 1 h.

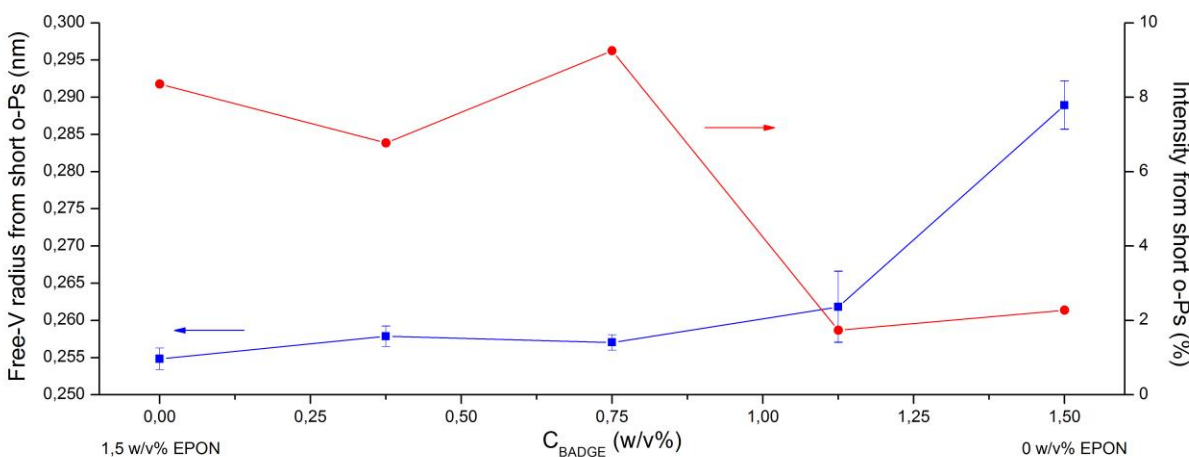


**Figure 17.** Free-volume element radius and intensity from the short o-Ps component as a function of BADGE concentration. The total amount of epoxy monomer was kept constant at 1.5 w/v%, so that 0 w/v% BADGE corresponds to 1.5 w/v% EPON, and vice versa (1 h reaction time, 1 w/v% TMHD).

The intensity of the short o-Ps component varies substantially between these samples, varying around 8% for the pure EPON membrane and the low BADGE concentrations, while dropping to ca. 2% for the higher concentrations. The high permeance and low retention observed for the latter two can thus mainly be ascribed to the size of the free-volume elements, rather than their abundance. However, it is perilous to correlate intensities with the

abundance of free-volume elements, as the intensity of a lifetime is also a function of the Ps formation probability. As the samples consist of different ratios of monomers, the formation probability, which is a function of the chemical environment [35], is probably not constant and hence no correlations between intensity and porosity can be made with high certainty.

Regarding the “long” lifetimes of epoxy-blending series, no clear trend is observed (**Figure 18**). This is possibly due to the very low intensity of this signal (below 0.5% for all samples), which decreases the certainty of the fitted lifetime. The correlation between the filtration results and the o-Ps lifetime is thus mainly determined by the short component, rather than by the long one. However, it can be concluded that the presence of BADGE in the organic solution, at every concentration, causes the formation of overall bigger free-volume elements (both those related to o-Ps short and o-Ps long). Furthermore, the size of the RB dye is similar to the size of the bigger free-volume elements, possibly explaining why the dye could not be completely rejected. However, the substantial retention of the smaller dyes (BTB and MO) leads to the hypothesis that other retention mechanisms than size exclusion, such as swelling and electrostatic repulsion, probably also play a role in the final membrane performance. Unfortunately, these mechanisms cannot be verified with PALS.

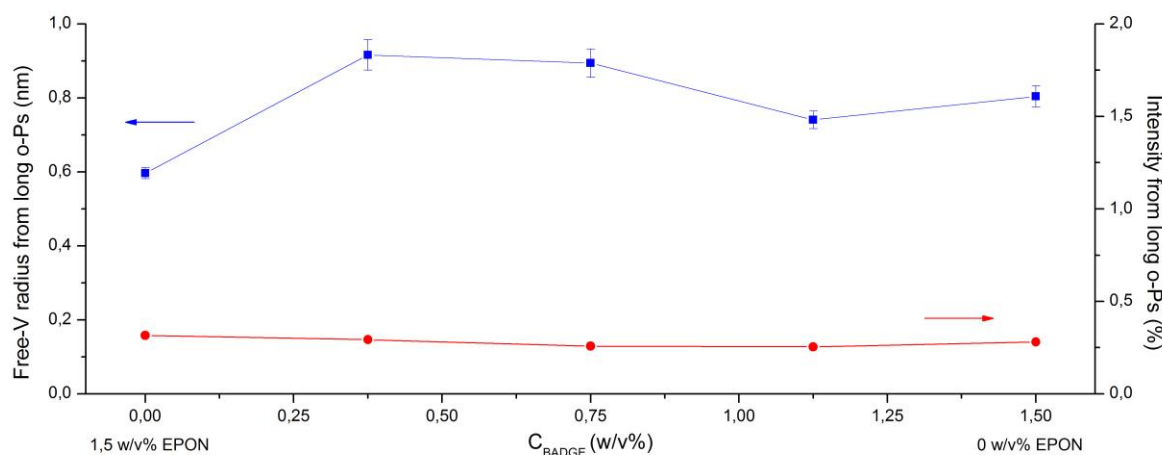


**Figure 18.** Free-volume element radius and intensity from the long o-Ps component as a function of BADGE concentration. The total amount of epoxy monomer was kept constant at 1.5 w/v%, so that 0 w/v% BADGE corresponds to 1.5 w/v% EPON, and vice versa (1 h reaction time, 1 w/v% TMHD).

#### 4. Stability tests

The chemical stability of the poly(epoxyether) membranes is expected to be superior to many other chemistries thanks to the stable ether bonds the top-layer is comprised of. In order to experimentally assess this theoretic stability, commonly encountered harsh conditions occurring in aqueous membrane environments were applied to the optimal membranes. Extreme pH conditions (pH 1 and pH 13, contact time of 48 h) were chosen to mimic feed streams from e.g. the mining industry, or cleaning conditions from food or beverage industries [36]. Stability against oxidants was studied by immersing the membrane in a 500 ppm NaOCl

solution at pH 4 during 2.5 h, conditions which are known to be more stringent than commonly encountered during accidental chlorination in a water treatment plant [37].

#### 4.1.1. EPON-based TFC-membranes

The optimal EPON-based TFC membrane (*i.e.* 1.5 w/v% EPON, 1 w/v% TMHD, 1 h reaction time) remains stable in both oxidizing and acid environments, as depicted by similar or even improved performances after the treatments (**Figure 19**). This remarkable chemical stability of the poly(epoxyether)-based top-layer is also largely superior to conventional polyamide-based TFC-membranes, as the performance of PA-membranes drastically changes or is completely lost under these conditions [38,39]. Additionally, an improved performance after NaOCl exposure was observed, attaining 98.7 ( $\pm 0.5$ )% RB retention, actually being the highest achieved retention in this work. The reason for the increase in membrane retention of these TFC membranes after chlorination is not fully understood, but the same effect is observed for PA-based top-layers [19,40–42]. Chlorination is sometimes even used as a strategy to boost or tailor their performance [40,43–47], but also for these conventional membranes, the exact mechanism behind the improvement is still not fully clarified [47].

Even though performance remained quasi unaltered after acid and chlorine exposure, changes in top-layer morphology are visible (**Figure S11**). After chlorine-treatment, larger and fused spheres occurred, while after acid-treatment, less and flattened spheres were present. These results indicate the flexibility of these membranes to retain their separation capacity while undergoing morphological alternations.

In caustic conditions, the membrane support-layer (*i.e.* XL-PI) did not remain stable, probably due to NaOH-mediated hydrolysis of the amide bonds [48], which originate after cross-linking the PI network [17]. Therefore, stability tests in caustic conditions could not be executed on any of the TFC-membranes, inviting the use of other supports for future IIP-synthesized membranes.

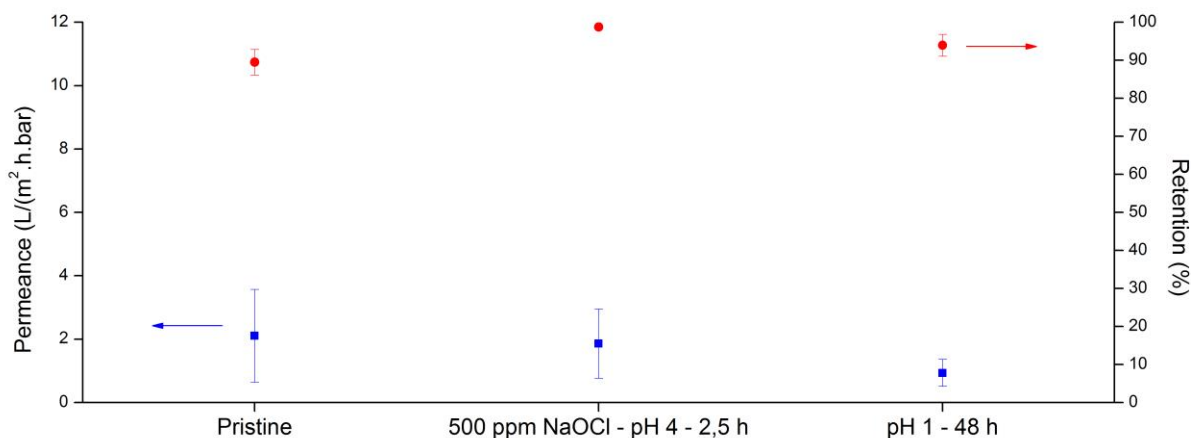


**Figure 19.** Stability of the pristine 1.5 w/v% EPON-based TFC-membrane (1 w/v% TMHD, 1 h reaction time), or after immersion in a 500 ppm aqueous NaOCl solution at pH 4 for 2.5 h or in an acid solution of pH1 for 48 h.

#### 4.1.2. EPON-BADGE-blend TFC-membranes

Also for the optimal TFC membrane, synthesized with both EPON and BADGE monomers (0.75/0.75 EPON/BADGE w/v%, 1 w/v% TMHD, 2 h reaction time), full stability in oxidizing environments is obtained (**Figure 20**). However, in acid environments, the membrane lost its separation capacity, as RB retention decreased and water permeance strongly increased, as opposed to the pure-EPON membrane. Theoretically, ether bonds are highly stable in acidic environments and are only cleaved with concentrated acids (usually HBr or HI) under high temperature [10]. However, here, the ether bond adjacent to the aromatic ring (indicated with arrows in **Figure S1**) is more susceptible to acid-mediated cleavage as it produces a better leaving group (i.e. stronger acid or weaker conjugated base), compared to aliphatic ethers. This cleavage will have a bigger impact on the poly(epoxyether) network if the bi-functional BADGE monomer is present, as cleavage of one ether bond results in the loss of cross-linking, while, three other linkages can compensate this for the tetra-functional EPON. This is why acid-resistance under the applied conditions was obtained for the pure EPON-based top-layer and not for the blended one. However, it is hypothesized that a full long term stability in acid conditions cannot be guaranteed for neither of these membranes due to their intrinsic chemical structure.

Regarding the top-layer morphology, fewer and less pronounced spheres are visible after chlorination and after acid treatment (**Figure S12**). However, the acid immersion step also induced cracks in the spheres (**Figure S13**), substantiating the lost separation capacity of this membrane.

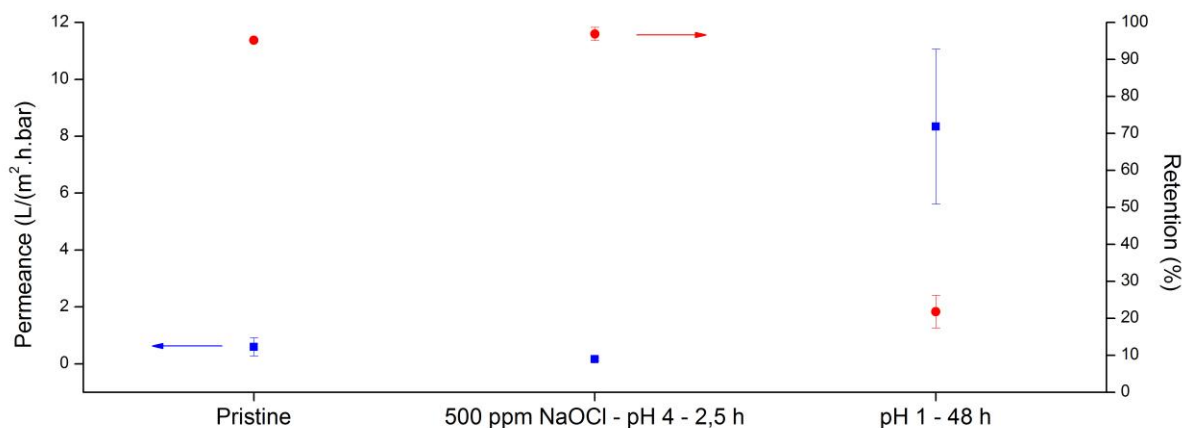


**Figure 20.** Stability of the pristine 0.75/0.75 EPON/BADGE w/v% -based TFC-membrane (1 w/v% TMHD, 2 h reaction time), or after immersion in an aqueous NaOCl solution (500 ppm) at pH 4 for 2.5 h or in an acid solution of pH 1 for 48 h.

## 5. Conclusions

The vast know-how about the bulk chemistry of epoxy resins was transferred for the first time to the interfacial synthesis of a robust poly(epoxyether) top-layer for TFC-membranes. A novel synthesis technique, called interfacial initiation of polymerization (IIP), was introduced

and resulted in dense and chemically resistant top-layers, achieving RB retentions of around 90%, MO retentions of 70% with reasonable water permeances ( $>2 \text{ Lm}^{-2}\text{h}^{-1}\text{bar}^{-1}$ ). A reaction time of 1 h was found to be the optimum for the explored EPON-based network. Correlations between ATR-FTIR, PALS, SEM and performance results were found, demonstrating the feasibility and reproducibility of this innovative membrane synthesis technique. Additionally, their proven stability in oxidizing (500 ppm NaOCl, pH 4, 2.5 h) and acidic conditions (pH 1, 48 h) and expected resistance in caustic conditions (provided an equally robust support layer) opens immense possibilities with respect to chemical cleaning and novel membrane applications. In general, the plethora of available epoxy monomers, reaction temperatures, reaction initiators and catalysts, as well as the use of other membrane supports, ensures high tunability in terms of final membrane performance, morphology and synthesis time. The IIP-synthesized poly(epoxyether) top-layers may therefore lay the foundation for a new generation of exceptionally stable (SR or ST)NF TFC-membranes.

## 6. Acknowledgements

This work is based upon experiments performed at the PLEPS instrument at the NEPOMUC facility operated by FRM II at the Heinz Maier-Leibnitz Zentrum (MLZ), Garching, Germany. The authors are grateful to KU Leuven for support through OT/11/061, as well as the IAP 6/27 on Functional Supramolecular systems of the Belgian Federal Government. R.V. thanks Research Foundation Flanders (FWO) for a SB-PhD fellowship (1S00917N). Maarten Bastin is thanked for the SEM images, Cédric Van Goethem and An Vandoren are kindly acknowledged for TEM sample preparation and imaging.

## 7. References

- [1] J.R. Werber, C.O. Osuji, M. Elimelech, Materials for next-generation desalination and water purification membranes, *Nat. Rev. Mater.* (2016) 16018. doi:10.1038/natrevmats.2016.18.
- [2] G.M. Geise, H.S. Lee, D.J. Miller, B.D. Freeman, J.E. McGrath, D.R. Paul, Water purification by membranes: The role of polymer science, *J. Polym. Sci. Part B Polym. Phys.* 48 (2010) 1685–1718. doi:10.1002/polb.22037.
- [3] S. Hermans, H. Mariën, C. Van Goethem, I.F.J. Vankelecom, Recent developments in thin film (nano)composite membranes for solvent resistant nanofiltration, *Curr. Opin. Chem. Eng.* 8 (2015) 45–54. doi:10.1016/j.coche.2015.01.009.
- [4] N. Fridman-Bishop, V. Freger, What Makes Aromatic Polyamide Membranes Superior: New Insights into Ion Transport and Membrane Structure, *J. Memb. Sci.* 540 (2017) 120–128. doi:10.1016/j.memsci.2017.06.035.
- [5] J.E. Cadotte, Interfacially Synthesized Reverse Osmosis Membrane, U.S. Patent No. 4,277,344, 1981.
- [6] P. Marchetti, M.F.J. Solomon, G. Szekely, A.G. Livingston, Molecular Separation with Organic Solvent Nano filtration : A Critical Review, *Chem. Rev.* 114 (2014) 10735–10806. doi:10.1021/cr500006j.
- [7] J.P. Pascault, R.J.J. Williams, General Concepts about Epoxy Polymers, 2010. doi:10.1002/9783527628704.ch1.
- [8] B. Ellis, Chemistry and Technology of Epoxy Resins, 1993. doi:10.1007/978-94-011-2932-9.
- [9] L.G. Wade, Organic Chemistry, 2013.
- [10] M.R. Thornton, R.N. Boyd, Organic Chemistry, 1992.
- [11] P. Vandezande, L.E.M. Gevers, I.F.J. Vankelecom, Solvent resistant nanofiltration: separating on a molecular level., *Chem. Soc. Rev.* 37 (2008) 365–405.

doi:10.1039/b610848m.

- [12] M. Bastin, E. Dom, K. Bogaert, S. Rutten, J. Van den Bosch, S. Hermans, G. Koeckelberghs, I.F.J. Vankelecom, Solvent tolerant nanofiltration membrane development using epoxy ring opening reactions, in: *Euromembrane 2018 Val.*, 2018.
- [13] I.E. Dell'Erba, R.J.J. Williams, Homopolymerisation of Epoxy Monomers Initiated by 4-(Dimethylamino)pyridine, *Polym. Eng. Sci.* 46 (2006) 351–359. doi:10.1002/pen.
- [14] J.P. Pascault, R.J.J. Williams, *Epoxy polymers: New Materials and Innovations*, 2010. doi:10.1007/BF01983263.
- [15] Momentive Specialty Chemicals Inc, *EPON™ and EPI-REZ™ Epoxy Resins*, 2013.
- [16] A.K. Holda, I.F.J. Vankelecom, Understanding and guiding the phase inversion process for synthesis of solvent resistant nanofiltration membranes, *J. Appl. Polym. Sci.* 132 (2015) 1–17. doi:10.1002/app.42130.
- [17] K. Vanherck, P. Vandezande, S.O. Aldea, I.F.J. Vankelecom, Cross-linked polyimide membranes for solvent resistant nanofiltration in aprotic solvents, *J. Memb. Sci.* 320 (2008) 468–476. doi:10.1016/j.memsci.2008.04.026.
- [18] P. Vandezande, L.E.M. Gevers, J.S. Paul, I.F.J. Vankelecom, P.A. Jacobs, High throughput screening for rapid development of membranes and membrane processes, *J. Memb. Sci.* 250 (2005) 305–310. doi:10.1016/j.memsci.2004.11.002.
- [19] R. Verbeke, V. Gomez, T. Koschine, S. Eyley, A. Szymczyk, M. Dickmann, T. Stimpel-Lindner, W. Egger, W. Thielemans, I. Vankelecom, Real-scale chlorination at pH4 of BW30 TFC membranes and their physicochemical characterization, *J. Memb. Sci.* 551 (2018) 123–135. doi:10.1016/j.memsci.2018.01.019.
- [20] S.J. Tao, Positronium Annihilation in Molecular Substances, *J. Chem. Phys.* 56 (1972) 5499–5510. doi:http://dx.doi.org/10.1063/1.1677067.
- [21] M. Eldrup, D. Lightbody, J.N. Sherwood, The temperature dependence of positron lifetimes in solid pivalic acid, *Chem. Phys.* 63 (1981) 51–58. doi:10.1016/0301-0104(81)80307-2.
- [22] C. Hugenschmidt, G. Dollinger, W. Egger, G. Kögel, B. Löwe, J. Mayer, P. Pikart, C. Piochacz, R. Repper, K. Schreckenbach, P. Sperr, M. Stadlbauer, Surface and bulk investigations at the high intensity positron beam facility NEPOMUC, *Appl. Surf. Sci.* 255 (2008) 29–32. doi:10.1016/j.apsusc.2008.05.304.
- [23] C. Hugenschmidt, C. Piochacz, M. Reiner, K. Schreckenbach, The NEPOMUC upgrade and advanced positron beam experiments, *New J. Phys.* 14 (2012). doi:10.1088/1367-2630/14/5/055027.
- [24] W. Egger, Pulsed low energy positron system (PLEPS) at the Munich research reactor

- FRM II, Phys. Status Solidi. 4 (2007) 3969–3972. doi:10.1002/pssc.200675812.
- [25] P. Sperr, W. Egger, G. Kögel, G. Dollinger, C. Hugenschmidt, R. Repper, C. Piochacz, Status of the pulsed low energy positron beam system (PLEPS) at the Munich Research Reactor FRM-II, Appl. Surf. Sci. 255 (2008) 35–38. doi:10.1016/j.apsusc.2008.05.307.
- [26] J. Algers, P. Sperr, W. Egger, G. Kögel, F. Maurer, Median implantation depth and implantation profile of 3–18 keV positrons in amorphous polymers, Phys. Rev. B. 67 (2003) 12–14. doi:10.1103/PhysRevB.67.125404.
- [27] P. Kirkegaard, J. V Olsen, M.M. Eldrup, PALSfit3: A software package for analysing positron lifetime spectra A software package for analysing positron lifetime spectra, 2017.
- [28] R.M. Silverstein, F.X. Webster, D. Kiemle, E.J. Einholm, Spectrometric Identification of Organic Compounds, 7th Edition, 2005. doi:10.1006/jmra.1996.0145.
- [29] L. Shao, L. Liu, S.-X. Cheng, Y.-D. Huang, J. Ma, Comparison of diamino cross-linking in different polyimide solutions and membranes by precipitation observation and gas transport, J. Memb. Sci. 312 (2008) 174–185. doi:10.1016/j.memsci.2007.12.060.
- [30] B. Schrader, Infrared and Raman Spectroscopy-Methods and Applications, 1994. doi:10.1016/0924-2031(00)00065-5.
- [31] F. Pacheco, R. Sougrat, M. Reinhard, J.O. Leckie, I. Pinnau, 3D visualization of the internal nanostructure of polyamide thin films in RO membranes, J. Memb. Sci. 501 (2016) 33–44. doi:10.1016/j.memsci.2015.10.061.
- [32] Y. Kourde-Hanafy, P. Loulergue, A. Szymczyk, B. Van Der Bruggen, M. Nachtnebel, M. Rabiller-baudry, J.-L. Audic, P. Pölt, K. Baddari, Influence of PVP content on degradation of PES/PVP membranes: Insights from characterization of membranes with controlled composition, J. Memb. Sci. 533 (2017) 261–269. doi:10.1016/j.memsci.2017.03.050.
- [33] R. Zimmermann, U. Freudenberg, R. Schweiß, D. Küttner, C. Werner, Hydroxide and hydronium ion adsorption — A survey, Curr. Opin. Colloid Interface Sci. 15 (2010) 196–202. doi:10.1016/j.cocis.2010.01.002.
- [34] R.W. Baker, Membrane Technology and Applications, John Wiley & Sons, Ltd, Chichester, UK, 2012.
- [35] O.E. Mogensen, Positron Annihilation in Chemistry, (1995) 268.
- [36] M. Paul, S.D. Jons, Chemistry and fabrication of polymeric nanofiltration membranes: A review, Polymer (Guildf). 103 (2016) 417–456. doi:10.1016/j.polymer.2016.07.085.
- [37] J.M. Gohil, A.K. Suresh, Chlorine Attack on Reverse Osmosis Membranes: Mechanisms and Mitigation Strategies, J. Memb. Sci. 541 (2017) 108–126. doi:10.1016/j.memsci.2017.06.092.

- [38] V.T. Do, C.Y. Tang, M. Reinhard, J.O. Leckie, Effects of chlorine exposure conditions on physicochemical properties and performance of a polyamide membrane-mechanisms and implications, *Environ. Sci. Technol.* 46 (2012) 13184–13192. doi:10.1021/es302867f.
- [39] J. Luo, Y. Wan, Effects of pH and salt on nanofiltration-a critical review, *J. Memb. Sci.* 438 (2013) 18–28. doi:10.1016/j.memsci.2013.03.029.
- [40] R. Verbeke, V. Gómez, I.F.J. Vankelecom, Chlorine-resistance of reverse osmosis (RO) polyamide membranes, *Prog. Polym. Sci.* 72 (2017) 1–15. doi:10.1016/j.progpolymsci.2017.05.003.
- [41] Y.N. Kwon, J.O. Leckie, Hypochlorite degradation of crosslinked polyamide membranes. II. Changes in hydrogen bonding behavior and performance, *J. Memb. Sci.* 282 (2006) 456–464. doi:10.1016/j.memsci.2006.06.004.
- [42] Y.N. Kwon, C.Y. Tang, J.O. Leckie, Change of membrane performance due to chlorination of crosslinked polyamide membranes, *J. Appl. Polym. Sci.* 102 (2006) 5895–5902. doi:10.1002/app.25071.
- [43] S.D. Jons, K.J. Stutts, M.S. Ferritto, W.E. Mickols, Treatment of composite polyamide membranes to improve performance. Patent Nr°5876602, 1999. doi:10.1016/S0958-2118(00)80090-7.
- [44] O. Coronell, B.J. Mariñas, D.G. Cahill, Depth heterogeneity of fully aromatic polyamide active layers in reverse osmosis and nanofiltration membranes, *Environ. Sci. Technol.* 45 (2011) 4513–4520. doi:10.1021/es200007h.
- [45] X. Zhai, J. Meng, R. Li, L. Ni, Y. Zhang, Hypochlorite treatment on thin film composite RO membrane to improve boron removal performance, *Desalination.* 274 (2011) 136–143. doi:10.1016/j.desal.2011.02.001.
- [46] N.Y. Yip, A. Tiraferri, W.A. Phillip, J.D. Schi, L.A. Hoover, Y.C. Kim, M. Elimelech, Thin-Film Composite Pressure Retarded Osmosis Membranes for Sustainable Power Generation from Salinity Gradients, (2011) 4360–4369. doi:10.1021/es104325z.
- [47] N.Y. Yip, M. Elimelech, Performance limiting effects in power generation from salinity gradients by pressure retarded osmosis, *Environ. Sci. Technol.* 45 (2011) 10273–10282. doi:10.1021/es203197e.
- [48] J. Clayden, N. Greeves, S. Warren, *Organic Chemistry*, 2012. doi:9780470401415.

**Highlights:**

- Well-known bulk chemistry of epoxy resins was transferred to the interfacial synthesis of TFC membranes
- Synthesis occurred via interfacial initiation of polymerization rather than via interfacial polymerization
- A chemically robust nanofiltration membrane was achieved, with 90% Rose Bengal (1017 Da) retention, 70% Methyl Orange (327 Da) retention and water fluxes  $> 2 \text{ Lm}^{-1}\text{h}^{-1}\text{bar}^{-1}$
- Stability in pH 1 (immersion for 48 h) and 500 ppm NaOCl (pH4, 500 ppm, immersion for 2.5h) was achieved

Accepted manuscript